Journal of Alloys and Compounds 509 (2011) 859–863

Contents lists available at ScienceDirect

Journal of Alloys and Compounds

journal homepage: www.elsevier.com/locate/jallcom

Sol–gel synthesis and thermal stability of luminescence of $Lu_3Al_5O_{12}:Ce^{3+}$ nano-garnet

R. Praveena[a], Liang Shi[a], Kyoung Hyuk Jang[a], V. Venkatramu[b], C.K. Jayasankar[c], Hyo Jin Seo[a,*]

[a] Department of Physics, Pukyong National University, 599-1, Daeyeon 3-Dong, Namgu, Busan 608 737, Republic of Korea
[b] Department of Physics, Yogi Vemana University, Kadapa 516 003, India
[c] Department of Physics, Sri Venkateswara University, Tirupati 517 502, India

ARTICLE INFO

Article history:
Received 11 February 2010
Received in revised form
18 September 2010
Accepted 22 September 2010
Available online 1 October 2010

Keywords:
Cerium ion
Lutetium aluminum nano-garnets
Photoluminescence
Thermal stability

ABSTRACT

Ce^{3+}-doped lutetium aluminum (LuAG) nano-garnet powder has been prepared by Pechini sol–gel method and characterized by X-ray diffraction, transmission electron microscope, excitation and photoluminescence spectra and decay measurements. The thermal stability of luminescence of the LuAG:Ce^{3+} has been evaluated for the temperature range 25–150 °C under the 460 nm excitation. The results indicate that the thermal stability of LuAG:Ce^{3+} is better than that of commercially available YAG:Ce^{3+} nano-garnet. The CIE chromaticity co-ordinates have been found to remain constant with change in temperature. Hence, it could be an apt candidate for generating white light when coupled to a blue LED.

1. Introduction

White light-emitting diodes (WLEDs) are emerging as an indispensable solid state light source for the next generation lighting industry and display systems due to their unique properties such as energy saving, environment-friendliness, small volume and long persistence. The major challenges in WLEDs are to achieve high luminous efficiency, high chromatic stability, good color rending properties and price competitiveness against fluorescent lamps. A comprehensive understanding of the nature and limitations of phosphors and the factors dominating the general trends in WLEDs is essential for advancing technological applications. There is a considerable interest in the development of WLEDs using a GaN as well as InGaN chip [1,2]. Therefore, the WLEDs require phosphors with efficient absorption bands in the near ultraviolet (NUV) region (λ_{ex} = 365–410 nm) or blue region (λ_{ex} = 420–480 nm). At present, rare earth based phosphors with efficiencies close to the theoretical maximum (100%) are employed in different fluorescent tubes, X-ray imaging and color televisions. Such applications depend on the luminescent properties of rare earth ions, e.g., sharp lines, high efficiency and high lumen equivalence [3]. Recently, the WLEDs composed of blue LED and a yellow YAG:Ce^{3+} nano-garnet have been investigated extensively due to their wide applications, such as back lighting for liquid-crystal displays and incandescent lamps [4–11]. These applications are particularly useful for saving electric power owing to the lower-energy consumption of LEDs. However, this WLED has a disadvantage of thermal degradation which is caused by heat generation of LED chip [12–14]. As a result, it catches up with the degradation of luminous intensity and the change of emission color.

Lutetium aluminum garnet ($Lu_3Al_5O_{12}$, LuAG) is not only isostructural to the YAG but also Ce^{3+} doped LuAG has already been recognized as optical material and scintillator [15,16]. In comparison with YAG:Ce, LuAG:Ce single crystals and single crystalline films show larger absorption co-efficient of ionizing radiation with higher quantum yields [17,18]. The concentration dependent photoluminescence (PL) and radioluminescence properties of Ce^{3+}-doped LuAG nano-garnets prepared by sol–gel combustion process have been reported [19–21]. Zhong et al. [22] synthesized Ce^{3+}-doped LuAG garnets by sol–gel process and studied the influence of annealing temperature and active ion concentration on luminescent properties and defects. Wang et al. [23] prepared Ce^{3+}-doped YAG and LuAG nano-garnet powder by co-precipitation method and studied their photoluminescence spectra under VUV excitation. Potdevin et al. [24] reported Ce^{3+}-doped YAG and LuAG garnets by sol–gel route from alkoxide precursors and analysed their excitation and luminescence spectra. Very recently, LuAG:Ce^{3+} nano-garnet powders also prepared by mixed

* Corresponding author.
E-mail address: hjseo@pknu.ac.kr (H.J. Seo).

0925-8388/$ – see front matter © 2010 Elsevier B.V. All rights reserved.
doi:10.1016/j.jallcom.2010.09.113

solvo-thermal method and studied concentration dependent luminescence properties [25]. However, the use of garnet phosphors in lighting applications also requires the detailed spectroscopic investigations on color characteristics. The degradation of luminescence efficiency and shift of chromaticity [26] for the WLEDs are the key issues because of increase of junction temperature. So, when the WLED phosphors are under investigation, thermal stability of luminescence is also important and has to be optimized [27,28]. High performance phosphors with high efficiency, high stability and low-temperature quenching are required. So far, there has been no report on temperature dependent luminescence of LuAG:Ce^{3+} nano-garnets.

In the present study, the LuAG:Ce^{3+} nano-garnet powder was prepared by Pechini sol–gel method. The temperature dependent PL spectra have been carried out from room temperature (RT) to 150 °C at 460 nm excitation. The decay curves and their lifetimes have been measured as a function of temperature with 355 nm excitation. Thermal stability of LuAG:Ce^{3+} nano-garnet has been evaluated by the dependence of PL intensities and the color coordinates with respect to temperature. This could be helpful in understanding the mechanisms responsible for the quenching of luminescence at high temperatures in developing new materials for WLED applications.

2. Experimental details

Lutetium aluminum nano-garnet of composition $Lu_{2.97}Ce_{0.03}Al_5O_{12}$ (the concentration of Ce^{3+} was 1.0 mol% with respect to Lu^{3+}) has been prepared by the sol–gel process described elsewhere [29]. The starting reagents are $Al(NO_3)_3$ (Aldrich, 99.999%), $Lu(NO_3)_3$ (Aldrich, 99.999%), $Ce(NO_3)_3$ (Aldrich, 99.9%), citric acid (Fluka, 99.5%) and poly ethylene glycol (Spectra Tech. Inc.). Stoichiometric molar ratio of high-purity $Lu(NO_3)_3$, $Al(NO_3)_3$ and $Ce(NO_3)_3$ materials were dissolved in 1 M HNO_3 under stirring. Then citric acid was added to the above solution during stirring. Finally, poly ethylene glycol (PEG) was added as a cross-linking agent. The molar ratio of metal ions to citric acid and to PEG was 1:2:8. The solution was stirred for 2 h and then dried at 90 °C for 36 h. The obtained gel was fired at 500 °C for 2 h in order to remove the residual nitrates and organic compounds. Finally, the powder sample was annealed at 900 °C for 16 h in air.

The XRD pattern of LuAG:Ce^{3+} nano-garnet was recorded on *X′ PERT PRO* X-ray diffractometer with Cu Kα (1.5406 Å) radiation in the range of $2\theta = 10–70°$. The morphology of LuAG:Ce^{3+} nano-garnet was examined by a Philips CM20 Transmission Electron Microscope (TEM) with an accelerating voltage up to 200 kV. The PL spectrum of LuAG:Ce^{3+} nano-garnet was recorded on a Photon Technology International (PTI) fluorimeter equipped with a Xe-arc lamp of power 60 W at RT. An argon ion laser (460 nm) equipped with a simple self-made heat cell was used to measure the temperature dependent PL spectra from RT to 150 °C. The decay curves were measured with a third harmonic (355 nm) pulsed Nd:YAG laser (Spectron Laser Sys. SL802G). The fluorescence was dispersed by a 75 cm monochromator (Acton Research Corp. Pro-750) and detected with a Hamamtsu R928 photomultiplier tube (PMT). The pulse width of the laser used for the decay time measurements is 5 ns and the instrumental response to the excitation pulse is less than 6 ns.

3. Results and discussion

Fig. 1 presents the XRD spectrum of (a) JCPDS data of LuAG host and (b) Ce^{3+}-doped LuAG nano-garnet powder. All peaks are well indexed to the $Lu_3Al_2Al_3O_{12}$ phase (JCPDS card No. 18-0761). The doped Ce^{3+} ions do not induce any significant phase change. The

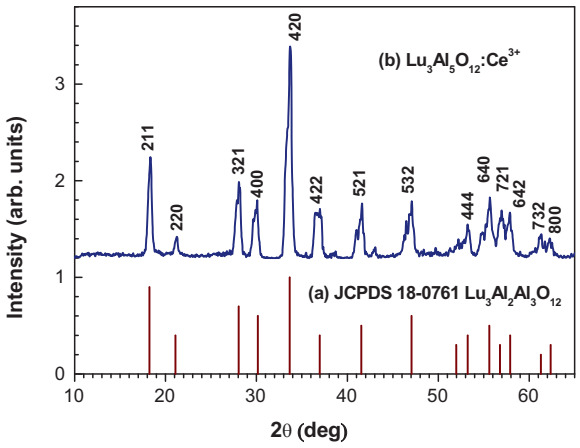

Fig. 1. XRD patterns of (a) JCPDS data of LuAG host and (b) LuAG:Ce^{3+} nano-garnet powder.

well-defined Bragg reflections in Fig. 1 indicate that the specimen under study is a well-crystallized single-phase of cubic structure [30]. The average crystallite size has been estimated from the full width at half maximum (FWHM) of the diffraction peak by the Scherrer's equation [31,32],

$$D_{hkl} = \frac{k\lambda}{\beta(2\theta)\cos\theta} \quad (1)$$

where '$\beta(2\theta)$' is the FWHM of the pure diffraction profile in radians, 'k' is the 0.89, 'λ' is the wavelength of the Cu Kα (1.5406 Å), 'θ' is the diffraction angle and 'D_{hkl}' is the average diameter of the crystallite. From the above equation, the crystalline size of the LuAG:Ce^{3+} nano-garnet powder is found to be 35 nm. The lattice constant has been calculated according to the equation:

$$\frac{1}{d^2} = \frac{h^2 + k^2 + l^2}{a^2} \quad (2)$$

where 'd' is the interplanar distance, 'h, k, l' are the crystal indices (Miller indices) and 'a' is the lattice constant. On the basis of the (4 2 0) crystal plane ($d = 2.65228$ Å in Fig. 1), the lattice constant is found to be 11.86 Å. A TEM micrograph of the LuAG:Ce^{3+} nano-garnet is shown in Fig. 2 and from which, morphologies and grain size for LuAG:Ce^{3+} nano-garnet have been understood and found that there are agglomerated particles with an average grain size of 22 nm. The aggregated particles could be due to the bridging of adjacent particles through the hydrogen bonding of water and the significant capillary action generated during the drying process in the precursors.

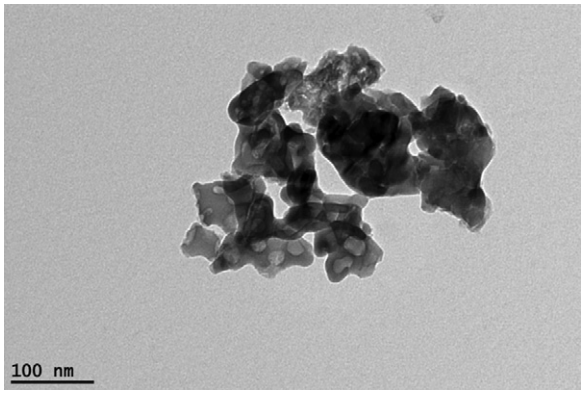

Fig. 2. TEM micrograph of LuAG:Ce^{3+} nano-garnet powder.

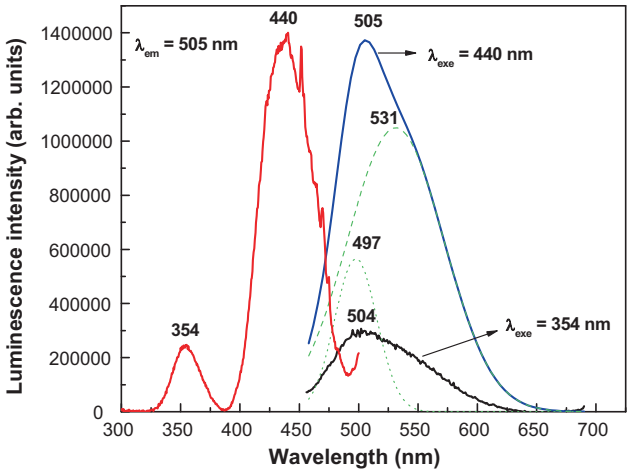

Fig. 3. RT excitation (λ_{em} = 505 nm) and PL (λ_{exe} = 354 and 440 nm) spectra of LuAG:Ce^{3+} nano-garnet. The PL spectrum attained under the 440 nm excitation has been deconvoluted into two peaks and are shown in dotted lines.

Fig. 3 shows the RT excitation (λ_{em} = 505 nm) and PL (λ_{ex} = 354 and 440 nm) spectra of the LuAG:Ce^{3+} nano-garnet. The excitation spectrum for Ce^{3+} contains two bands, namely, a weak band with a maximum at 354 nm and a strong band with a maximum at 440 nm. Ce^{3+} ion has only one electron in the 4f state and its ground state split into the $^2F_{7/2}$ and $^2F_{5/2}$ levels with an energy difference of about 2200 cm^{-1}. The next higher state originates from the 5d state and 4f–5d transitions are parity and spin allowed. The 5d state is strongly affected by crystal-field of the host matrix and split into several 5d sub-bands. Therefore, the two excitation bands are due to the absorption of the incident radiation by Ce^{3+} ions which leads to the excitation of electrons from the $4f^1$ ground state ($^2F_{5/2}$, $^2F_{7/2}$) to the excited $5d^1$ levels (^2D) [33]. The excitation band at 440 nm is most intense band and provides a strong basis to make use of this nano-garnet powder to InGaN based blue LED component for white light generation. The emission of commercially available blue LEDs is in the range of 420–480 nm. This is in perfect match with the excitation band of LuAG:Ce^{3+} nano-garnet as mentioned above.

The PL spectrum (Fig. 3) displays an apparent broad band covering from 450 to 650 nm with a maximum at around 505 nm, which is in good agreement with the RT PL spectrum of LuAG:Ce^{3+} single crystals and films [16,18]. The PL spectrum obtained under 440 nm excitation has been deconvoluted into two components centered at about 497 and 531 nm, respectively, shown in Fig. 3, which are similar to the PL spectrum of the LuAG:Ce single crystal films at 9 K [18]. Obviously, the emissions are ascribed to the electron transitions from the lowest crystal-field splitting component of the 5d level (^2D) to the ground state of Ce^{3+} ($^2F_{5/2}$, $^2F_{7/2}$) [34]. At RT, two emission lines overlap, resulting in a structureless band. On the other hand, it is observed that no changes in the shapes and ranges but changes are noticed in their intensities of the PL spectrum for different excitation wavelengths. Additionally, it is inspiring that the PL spectrum has been well matches with the sensitivity curve of Si-photodiode and CCD arrays that are the prime candidates as scintillation sensors in digital applications [35].

The excitation and PL spectra of LuAG:Ce^{3+} nano-garnet prepared by the Pechini sol–gel method are similar to the LuAG:Ce^{3+} nano-garnets prepared by sol–gel combustion method [19–21] except the difference between the energy positions of two bands in the excitation spectrum which is slightly decreased in the LuAG:Ce^{3+} nano-garnet prepared by the Pechini sol–gel method (5522 cm^{-1}) than that of the same prepared by sol–gel combustion method (6430 cm^{-1}) for the same emission at 505 nm. This could be due to the dependency of inter-configurational 4f–5d energies on the crystal-field of the host matrix since the 5d orbitals have a greater radial extension. This suggests that the Ce^{3+} ions experience weaker crystal-field in the LuAG:Ce^{3+} nano-garnet prepared by sol–gel technique than that of prepared by sol–gel combustion method. On the other hand, the energy splitting of the 5d state in LuAG:Ce^{3+} is smaller than those in YAG:Ce^{3+} [23]. Moreover, the emission peak (at 560 nm) of YAG:Ce^{3+} nano-garnet [36] is red-shifted compared to that of LuAG:Ce^{3+} nano-garnet. This could be due to the well known fact that the positions of 5d energy levels of Ce^{3+} depend on the nephelauxetic effect (covalency), crystal-field splitting and the Stokes shift [37]. Potdevin et al. [24] also observed the shift in the excitation spectrum when Y^{3+} ions were replaced by Lu^{3+} ions due to the changes in the lattice parameter.

Garnets generate large crystal-field strengths. Therefore, Ce^{3+}-doped garnet-type phosphors emit in green–yellow spectral region, whereas other Ce^{3+}-doped phosphors emit in UV or blue spectral region. The covalent character and crystal-field strength can be increased by partial replacement of Al–O groups by Si–N [38]. Furthermore, Ce^{3+} ion occupies different sites in the garnet phosphors. The changes in emission and excitation for Ce^{3+} garnet phosphors through compositional modifications have been documented in the literature for dodecahedral, octahedral and tetrahedral site modifications [39,40]. Setlur and Srivastava [38] observed that there are at least two types of Ce^{3+} ions in the LuAG:Ce^{3+} nano-garnet. They discussed about the high and low energy sites occupied by the Ce^{3+} ion in the garnet phosphors and studied the energy transfer between intrinsic higher energy Ce^{3+} sites and lower energy Ce^{3+} traps. However, site selective laser spectroscopy could give further insights towards the excitation and emission of different Ce^{3+} centers as well as the energy transfer processes which is beyond the scope of this paper.

High-power WLEDs require a lower thermal quenching to keep the chromaticity and the bright white light output. Fig. 4(a) shows the temperature dependent PL spectra of LuAG:Ce^{3+} nano-garnet excited by 460 nm. The variation of PL intensities against temperature is plotted in Fig. 4(b). It is well known that the temperature of an LED package rises because of heat generation by the LED itself. The phosphors used for color conversion material of WLED are required to emit luminescence effectively up to 150 °C. From the Fig. 4(b), it can be observed that the PL intensity of LuAG:Ce^{3+} nano-garnet remains unchanged with increasing temperature. The data of $(Y,Gd)_3Al_5O_{12}$:Ce^{3+} (YAG:Ce^{3+}) nano-garnet [41] are also compared in Fig. 4(b). From Fig. 4(b), it is observed that the PL intensity of YAG:Ce^{3+} nano-garnet is reduced to ~75% of its initial intensity when the temperature is increased from RT to 170 °C. Zhang et al. [42] also observed that PL intensity of YAG:Ce^{3+} nano-garnet reduces by about 27% for 340 nm and 54% for 460 nm excitations when the temperature is increased from RT to 300 °C (573 K). Therefore, LuAG nano-garnet has an excellent thermal stability than that of YAG nano-garnet. This could be due to the thermal quenching is stronger when the PL spectrum of the nano-garnet is red shifted. Moreover, no shift and broadening of the PL peaks have been observed with increasing temperature (Fig. 4). This result is contradictory to the results obtained for M_2SiO_4:Eu^{2+} (M = Ca, Sr, Ba) and $Sr_3Al_2O_5Cl_2$:Ce^{3+},Li^+ phosphors in Refs. [28,43] where the shift and broadening of the PL peaks have been noticed with increasing temperature. This suggests again that the LuAG:Ce^{3+} nano-garnet exhibits good thermal stability.

The PL decay curves of LuAG:Ce^{3+} nano-garnet have been measured at different temperatures between 25 and 150 °C under the 355 nm excitation. Fig. 5 shows the decay curves at 25, 100 and 150 °C which exhibit non-exponential nature for all temperature range studied. These curves are well fitted into double exponential

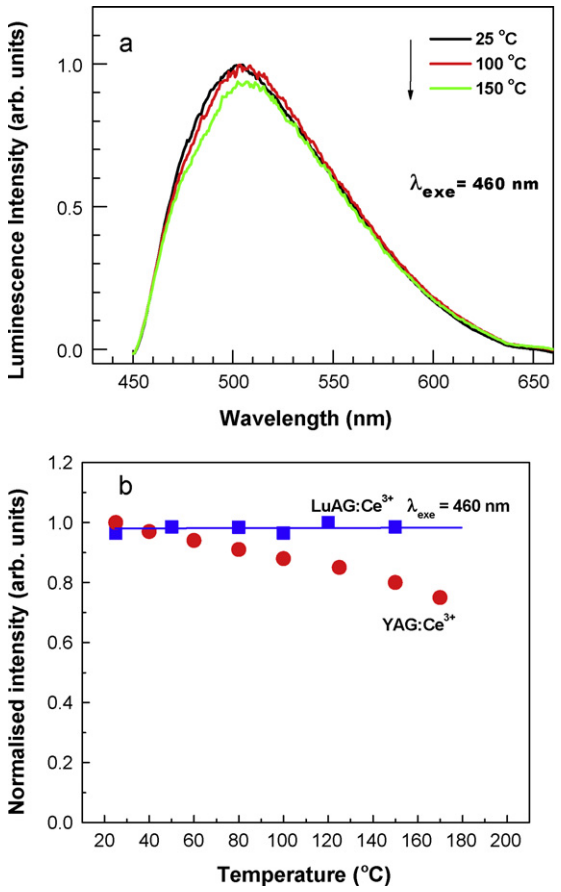

Fig. 4. (a) PL spectra at different temperatures under 460 nm excitation and (b) temperature dependent normalized integrated PL intensities of LuAG:Ce^{3+} nano-garnet. The data of YAG:Ce^{3+} nano-garnet are also compared in (b).

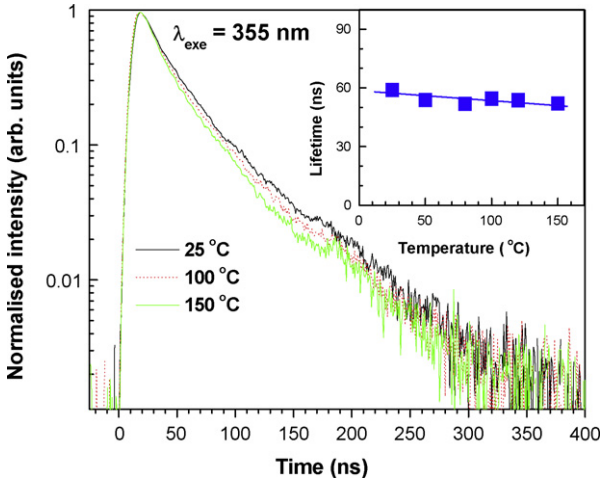

Fig. 5. The PL decay profiles of LuAG:Ce^{3+} nano-garnet at different temperatures. The inset shows the variation of lifetimes (τ_1) with respect to the temperature.

function:

$$I = I_0 + A_1 \exp\left(\frac{-t}{\tau_1}\right) + A_2 \exp\left(\frac{-t}{\tau_2}\right) \quad (3)$$

The values of τ_1 and τ_2 extracted from the fitted curves are presented in Table 1. The fast and slow components may be attributed to the radiative ($5d \rightarrow 4f^1$ transitions in Ce^{3+} ions) and the migration stages of excitation, respectively. The decay times for λ_{em} = 505 nm obtained in the present study are in reasonable agreement with

Table 1
Photoluminescence decay times of LuAG:Ce^{3+} nano-garnet powder at different temperatures.

Temperature (°C)	Lifetime (ns)	
	τ_1	τ_2
25	59	20
50	54	19
80	52	17
100	55	18
120	54	18
150	52	17

other reported LuAG:Ce^{3+} nano-garnets [38] whereas thrice as fast as those found for the LuAG:Ce^{3+} single crystals (63 and 288 ns) [44,45] and single crystalline films (50 and 158 ns) [44]. Compared with LuAG:Ce^{3+} single crystals and single crystalline films, the differences of the decay times are mainly due to the differences in microstructures between nano-garnet powders, single crystals and single crystalline films. Some authors reported that the radiative processes strongly depend on both the size and shape of the particles besides effective refractive index (n_{eff}) [46–48]. These types of studies are very interesting and will be focused in our future work.

The fast decay component of 20 ns (at RT) is inspiring and satisfies the requirement of fast scintillators and WLEDs. The values of τ_1 are plotted against the temperature and shown in the inset of Fig. 5. The lifetimes are decreasing slightly with increasing temperature due to the parity allowed 5d–4f transition of Ce^{3+} ion with high radiative probability. Generally, as the increase of temperature, the non-radiative processes will be more efficient and consequently the lifetime will be shorter [45]. Therefore, the temperature dependence of the lifetime is due to the increase in thermal assisted non-radiative transition probability.

Fig. 6 shows the CIE (1931) chromaticity co-ordinates of LuAG:Ce^{3+} nano-garnet from 25 to 150 °C under 460 nm excitation. The color co-ordinates at RT are estimated as $x = 0.3455$, $y = 0.5298$, correspond to correlated color temperature (CCT) of 5258 K which is nearer to that of the day light (5500 K) [49]. These color co-ordinates are very useful in determining the exact emission color of the sample. If a straight line is drawn between the co-ordinates of blue LED (λ_{em} = 450 nm) ($x = 0.15$, $y = 0.02$) and LuAG:Ce^{3+} nano-garnet, it passes very close to the "ideal white" ($x = 0.33$, $y = 0.33$)

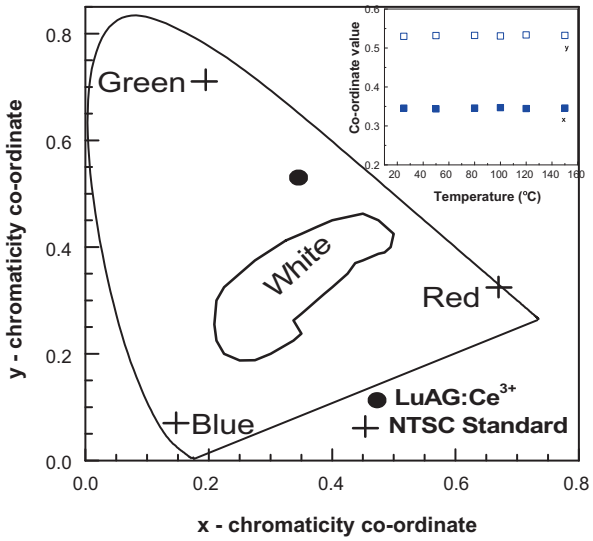

Fig. 6. CIE (1931) chromatic co-ordinates of LuAG:Ce^{3+} nano-garnet calculated from the PL spectra in Fig. 4. The inset shows the variation of x and y co-ordinate values as a function of temperature at 460 nm excitation.

site of the CIE chromaticity diagram. Moreover, the emission color remains constant from 25 to 150 °C (see the inset of Fig. 6), reducing the role of thermally activated processes. In the case of YAG:Ce^{3+} nano-garnet, the increase of temperature led to the quench in intensity and changes in the chromaticity of the WLED with as-prepared phosphors [42]. The above observations suggest that LuAG:Ce^{3+} nano-garnet can also be considered to develop white light from InGaN-based blue LED.

4. Conclusions

LuAG:Ce^{3+} nano-garnet powder was successfully synthesized and characterized by XRD, SEM, PL and decay measurements. The obtained powder is agglomerated with an average particle size of 22 nm. The PL spectrum is located in the green–yellow region. The temperature dependent PL spectra have been measured for the temperature range 25–150 °C. With the increase in the temperature up to 150 °C, the LuAG:Ce^{3+} nano-garnet showed good thermal luminescence stability under 460 nm. The fluorescence decay curves under 355 nm exhibit bi-exponential nature accompanied by slight decrease of lifetime due to increase in thermal assisted non-radiative transition probability. The quality of light has been evaluated using CIE chromaticity diagram. The present LuAG:Ce^{3+} nano-garnet exhibits stable color co-ordinates with respect to temperature. All these experimental results show that LuAG:Ce^{3+} nano-garnet has an excellent thermal stability than that of commercially available YAG:Ce^{3+} nano-garnet and can be used in the WLED applications.

Acknowledgements

This study was financially supported by Pukyong National University in the 2009 Post-Doc Program and by the Korea Science and Engineering Foundation (KOSEF) grant funded by the Korea government (Ministry of Education, Science and Technology; MEST) (No. 2009-0078682). CKJ is grateful to Defense Research and Development Organization (DRDO), Government of India for the award of the Major Research Project (ERIP/ER/0303438/M/01, dt. 20-12-2004).

References

[1] Z. Wang, N. Xiang, Q. Wang, G. Zhang, M. Gong, J. Lumin. 130 (2010) 35.
[2] S. Nakamura, MRS Bull. 34 (2009) 101.
[3] Q.Y. Zhang, X.Y. Huang, Prog. Mater. Sci. 55 (2010) 353.
[4] Z. Wu, X. Zhang, W. He, Y. Du, N. Jia, G. Xu, J. Alloys Compd. 468 (2009) 571.
[5] Q. Shao, H. Li, Y. Dong, J. Jiang, C. Liang, J. He, J. Alloys Compd. 498 (2010) 199.
[6] H.M.H. Fadlalla, C. Tang, J. Cryst. Growth 311 (2009) 3737.
[7] S. Mukherjee, V. Sudarsan, R.K. Vatsa, A.K. Tyagi, J. Lumin. 129 (2009) 69.
[8] A. Katelnikovas, H. Bettentrup, D. Uhlich, S. Sakirzanovas, T. Justel, A. Kareiva, J. Lumin. 129 (2009) 1356.
[9] H. Yang, D.-K. Lee, Y.-S. Kim, Mater. Chem. Phys. 114 (2009) 665.
[10] A. Katelnikovas, T. Bareika, P. Vitta, T. Justel, H. Winkler, A. Kareiva, A. Zukauskas, G. Tamulaitis, Opt. Mater. 32 (2010) 1261.
[11] K.Y. Jung, Y.C. Kang, Physica B 405 (2010) 1615.
[12] Y.F. Zhang, L. Li, X.S. Zhang, Q. Xi, J. Rare Earth 26 (2008) 446.
[13] A.A. Setlur, W.J. Heward, M.E. Hannah, U. Happek, Chem. Mater. 20 (2008) 6277.
[14] R.J. Xie, N. Hirosaki, Sci. Technol. Adv. Mater. 8 (2007) 588.
[15] V. Babin, V. Gorbenko, A. Krasnikov, A. Makhov, M. Nikl, S. Zazubovich, Yu. Zorenko, Radiat. Meas. 45 (2010) 415.
[16] J.A. Mares, A. Beitlerova, M. Nikl, N. Solovieva, C. D'Ambrosio, K. Blazek, P. Maly, K. Nejezchleb, F. de Notaristefani, Radiat. Meas. 38 (2004) 353.
[17] A. Koch, F. Peyrin, P. Heurtier, B. Ferrand, B. Chambaz, W. Ludwig, M. Couchaud, Proc. SPIE 3659 (1999) 170.
[18] Y. Zorenko, V. Gorbenko, I. Konstankevych, A. Voloshinovskii, G. Stryganyuk, V. Mikhailin, V. Volobanov, D. Spassky, J. Lumin. 114 (2005) 85.
[19] H.L. Li, X.J. Liu, L.P. Huang, Opt. Mater. 29 (2007) 1138.
[20] H.L. Li, X.J. Liu, Q. Zhang, L.P. Huang, J. Rare Earth 25 (2007) 401.
[21] X.J. Liu, H.L. Li, R.J. Xie, Y. Zeng, L.P. Huang, J. Lumin. 124 (2007) 75.
[22] Y.R. Zhong, R.S. Yu, Z.X. Li, B.Y. Wang, L. Wei, Mater. Sci. Forum. 607 (2009) 128.
[23] Z. Wang, M. Xu, W. Zhang, M. Yin, J. Lumin. 122–123 (2007) 437.
[24] A. Potdevin, G. Chadeyron, D. Boyer, R. Mahiou, Phys. Status Solidi C 4 (2007) 65.
[25] L. Wang, M. Yin, C. Guo, W. Zhang, J. Rare Earth 28 (2010) 16.
[26] R.J. Xie, N. Hirosaki, M. Mitomo, K. Sakuma, N. Kimura, Appl. Phys. Lett. 89 (2006) 241103.
[27] Y.S. Tang, S.F. Hu, C.C. Lin, C.B. Nitin, R.S. Liu, Appl. Phys. Lett. 90 (2007) 151108.
[28] J.S. Kim, Y.H. Park, S.M. Kim, J.C. Choi, H.L. Park, Solid State Commun. 133 (2005) 445.
[29] V. Venkatramu, D. Falcomer, A. Speghini, M. Bettinelli, C.K. Jayasankar, J. Lumin. 128 (2008) 811.
[30] POWDER Diffraction File: Release 1999, Pensylvannia: Joint Committee on Powder Diffraction Standards-International Center for Diffraction Data, c 1999, PDF numbers: 73-1368 and 82-0575, CD-ROM.
[31] J.J. Zhang, J.W. Ning, X.J. Liu, Mater. Lett. 57 (2003) 3867.
[32] N. Matsushita, N. Tsuchiya, K. Kanatsuka, J. Am. Ceram. Soc. 82 (1999) 1977.
[33] Y. Zhou, J. Lin, M. Yu, S. Wang, H. Zhang, Mater. Lett. 56 (2002) 628.
[34] J. Lin, Q. Su, J. Mater. Chem. 5 (1995) 1151.
[35] A. Lempicki, A.J. Wojtowicz, C. Brecher, in: S.R. Rotman (Ed.), Wide-Gap Luminescent Materials: Theory and Applications, Kluwer Academic Publishers, Norwell, MA, 1997, p. 235.
[36] D. Haranath, H. Chander, P. Sharma, S. Singh, Appl. Phys. Lett. 89 (2006) 173118.
[37] G. Blasse, B.C. Grabmaier, Luminescent Materials, Springer, Berlin/Heidelberg, 1994.
[38] A.A. Setlur, A.M. Srivastava, Opt. Mater. 29 (2007) 1647.
[39] J.M. Robertson, M.W. van Tol, W.H. Smits, J.P.H. Heynen, Philips J. Res. 36 (1981) 36.
[40] T.Y. Tien, E.F. Gibbons, R.G. DeLosh, P.J. Zacmanidis, D.E. Smith, H.L. Stadler, J. Electrochem. Soc. 120 (1973) 278.
[41] Y. Shimomura, T. Honma, M. Shigeiwa, T. Akai, K. Okamoto, N. Kijima, J. Electrochem. Soc. 154 (2007) J35.
[42] Y. Zhang, L. Li, X. Zhang, Q. Xi, J. Rare Earth 26 (2008) 446.
[43] X. Zhang, B. Park, N. Choi, J. Kim, G.C. Kim, J.H. Yoo, Mater. Lett. 63 (2009) 700.
[44] Yu.V. Zorenko, V.I. Gorbenko, G.B. Stryganyuk, V.N. Kolobanov, D.A. Spasskil, K. Nlazek, M. Nikl, Opt. Spectrosc. 99 (2005) 923.
[45] M. Nikl, E. Mihokova, J.A. Mares, A. Vedda, M. Martini, K. Nejezchleb, K. Blazek, Phys. Status Solidi A 181 (2000) R10.
[46] R.S. Meltzer, S.P. Feofilov, B. Tissue, H.B. Yuan, Phys. Rev. B 60 (1999) R14012.
[47] H.P. Christensen, D.R. Gabbe, H.P. Jenssen, Phys. Rev. B 25 (1982) 1467.
[48] J. Amami, D. Hreniak, Y. Guyot, W. Zhao, G. Boulon, J. Lumin. 130 (2010) 603.
[49] E.C. Fuchs, C. Sommer, F.P. Wenzl, B. Bitschnau, A.H. Paulitsch, A. Muhlanger, K. Gatterer, Mater. Sci. Eng. B 156 (2009) 73.